

Reovirus $\mu 2$ Protein Determines Strain-Specific Differences in the Rate of Viral Inclusion Formation in L929 Cells

J. L. Mbisa,* M. M. Becker,†‡ S. Zou,§ T. S. Dermody,†‡[¶] and E. G. Brown*¹

*Department of Biochemistry, Microbiology, and Immunology, Faculty of Medicine, University of Ottawa, Ottawa, Ontario K1H 8M5, Canada; and

†Department of Microbiology and Immunology, ‡Department of Pediatrics, and ¶Elizabeth B. Lamb Center for Pediatric Research, Vanderbilt University School of Medicine, Nashville, Tennessee 37232; and §Bloodborne Pathogens Division, Bureau of Infectious Diseases, Laboratory Center for Disease Control, Main Statistics Building, Tunney's Pasture, Ottawa, Ontario K1A 0K9, Canada

Received July 6, 1999; returned to author for revision August 19, 1999; accepted April 14, 2000

Reovirus infection induces the formation of large cytoplasmic inclusions that serve as the major site of viral assembly. Reovirus strains type 3 Dearing (T3D) and type 1 Lang (T1L) differ in the rate of inclusion formation in L929 cells. The median time of inclusion formation is 18 h in cells infected with T3D and 39 h in cells infected with T1L. Using reassortant viruses that contain combinations of gene segments derived from T1L and T3D, we found that the M1 gene, which encodes the $\mu 2$ protein, is the primary determinant of the rate of inclusion formation. The S3 gene, which encodes the nonstructural protein σNS , plays a secondary role in this process. The subcellular location of the $\mu 2$ protein was determined by confocal laser scanning microscopy using dual-fluorescence labeling of $\mu 2$ and the outer-capsid protein $\mu 1/\mu 1C$. In virus-infected cells, $\mu 2$ protein colocalized with other viral proteins in inclusions and was also distributed diffusely in the cytoplasm and nucleus. Expression of recombinant T1L and T3D $\mu 2$ proteins resulted in the formation of protein complexes resembling inclusions in both the cytoplasm and the nucleus with kinetics that reflected the strain of origin. The median time of $\mu 2$ protein complex formation was 22 h in cells transfected with the T3D M1 gene and 43 h in cells transfected with the T1L M1 gene. These findings suggest that the $\mu 2$ protein influences the rate of inclusion formation and contributes to inclusion morphogenesis. The requirement of $\mu 2$ protein in inclusion formation was tested by determining the subcellular localization of $\mu 2$ in cells infected with temperature-sensitive (ts) mutants that are defective in viral assembly. In contrast to infection with wild-type virus, $\mu 2$ did not colocalize with $\mu 1/\mu 1C$ protein in subcellular structures that formed in cells infected at nonpermissive temperature with ts mutants tsH11.2, tsC447, and tsG453 with mutations in the M1, S2, and S4 genes, respectively. These results suggest that despite the role of the $\mu 2$ protein in controlling the rate of inclusion formation, this process is a concerted function of several reovirus proteins. © 2000 Academic Press

INTRODUCTION

In association with the production of nucleic acid and protein, viral infection often involves the reorganization of cellular architecture to generate sites that facilitate viral assembly. All members of the *Reoviridae* induce cytoplasmic inclusions (Francki and Boccardo, 1983) that contain fibrillar constituents. In the case of orthoreoviruses, these filamentous structures have been identified as intermediate filament proteins (Sharpe *et al.*, 1982). Insect reoviruses (cypoviruses) encode a polyhedrin protein that forms the matrix of inclusions (Payne and Mertens, 1983). Viral proteins that mediate inclusion formation have not been identified for vertebrate reoviruses.

Mammalian reoviruses have a segmented genome consisting of 10 double-stranded (ds) RNA gene segments enclosed within a double-shelled capsid. Each segment encodes a single protein with the exception of S1, which is dicistronic (reviewed by Nibert *et al.*, 1996).

During viral entry into cells, the outer capsid is removed to produce transcriptionally active single-shelled, viral core particles. The resulting primary transcripts are translated to produce viral proteins that assemble with genomic sets of 10 mRNAs to produce replicase particles that synthesize minus-sense RNAs resulting in the formation of progeny dsRNA. Viral proteins and RNA are directed to inclusions that first appear by phase-contrast microscopy as dense granules scattered in the cytoplasm that coalesce around the nucleus later in infection (Sharpe *et al.*, 1982; Gomatos *et al.*, 1962). Reovirus inclusions are large cytoplasmic structures that are detectable by a variety of light and electron microscopic techniques (Zarbl and Millward, 1983). These inclusions are thought to be the primary sites of viral assembly since they contain paracrystalline arrays of virions late in infection (Gomatos *et al.*, 1962; Spendlove *et al.*, 1963; Dales *et al.*, 1965; Fields *et al.*, 1971).

Mechanisms by which viral proteins and RNA are directed to inclusions are not known. The involvement of host cytoskeletal proteins in reovirus inclusion formation and replication has previously been investigated. Reovi-

¹To whom correspondence and reprint requests should be addressed. Fax: (613) 562-5452. E-mail: ebrown@uottawa.ca.

rus infection of CV-1 cells results in disruption of the vimentin, intermediate filament network followed by its reorganization into a fibrous network within viral inclusions (Sharpe *et al.*, 1982). Microtubule and microfilament organization is not affected. However, virions and viral proteins appear to be attached to microtubules (Babiss *et al.*, 1979), which are thought to be involved in viral transport rather than morphogenesis. Colchicine treatment of reovirus-infected cells prevents development of large perinuclear inclusions without reducing viral yield (Babiss *et al.*, 1979; Spendlove *et al.*, 1964).

One of the three medium-sized gene segments, M1, encodes the $\mu 2$ protein, which is a minor component of the viral core. The $\mu 2$ protein is present in about 18 copies per virion (Coombs, 1998a) and is located in the viral core along with the viral polymerase at the base of the icosahedral vertices (Dryden *et al.*, 1998). Studies using reassortant viruses derived from reovirus strains type 1 Lang (T1L) and type 3 Dearing (T3D) have demonstrated that the $\mu 2$ -encoding M1 gene segregates with strain-specific differences in several biological properties including replication in myocardial cells (Matoba *et al.*, 1991), bovine aortic endothelial cells (Matoba *et al.*, 1993), and Madin–Darby canine kidney cells (Rodgers *et al.*, 1997). The M1 gene also segregates with strain-specific differences in induction of myocarditis (Sherry and Fields, 1989; Sherry and Blum, 1994; Sherry *et al.*, 1998) and hepatic injury (Haller *et al.*, 1995) in mice.

In addition to its role in reovirus growth in cell culture and pathogenesis in mice, the $\mu 2$ protein is involved in RNA synthesis. The M1 gene segment segregates with strain-specific differences in the temperature optimum of transcription, the extent of transcription (in conjunction with the L1 gene segment) (Yin *et al.*, 1996), and NTPase activity (Noble and Nibert, 1997). The M1 gene temperature-sensitive (ts) mutant tsH11.2 is defective in dsRNA synthesis, which suggests that the $\mu 2$ protein is required for genome replication (Coombs, 1996). Recombinant $\mu 2$ protein binds both single-stranded (ss) and dsRNA (Brentano *et al.*, 1998). The M1 genes of T1L and T3D contain a single open reading frame of 736 amino acids that corresponds to the $\mu 2$ protein. The deduced amino acid sequences of T1L and T3D $\mu 2$ proteins are very conserved, differing at only 10 amino acid positions (Wiener *et al.*, 1989; Zou and Brown, 1992, 1996b). These 10 amino acid differences must account for the differences in T1L and T3D attributable to the $\mu 2$ protein.

We conducted experiments to identify the genetic basis for inclusion formation in reovirus. Following the observation that T1L and T3D differ in the rate of inclusion formation we used reassortant viruses to identify viral genes that control this phenotype. We identified the M1 gene encoding the $\mu 2$ protein as the primary determinant in the rate of inclusion formation with a secondary role for the S3 gene encoding the nonstructural protein σ NS. The intracellular localization of $\mu 2$ protein

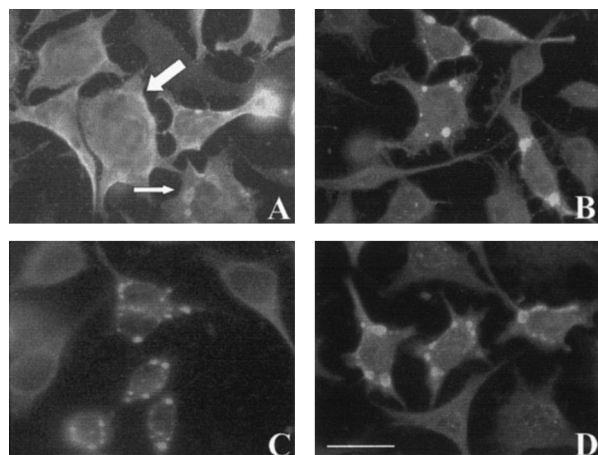


FIG. 1. Subcellular localization of reovirus proteins in cells infected with reovirus strains T1L or T3D. L929 cells were infected with T1L and labeled with rabbit anti-T1L antiserum at 24 (A) and 48 (C) h p.i. or with T3D and labeled with rabbit anti-T3D antiserum at 24 (B) and 48 (D) h p.i. Infections were done at an m.o.i. of 10 PFU per cell. The secondary antibody used was Cy3-conjugated donkey anti-rabbit antiserum. Images were obtained using an epifluorescence microscope. An antigen-positive cell without inclusions is indicated with a heavy arrow and a cell with inclusions is indicated with a thin arrow in (A). Bar represents 10 μ m.

was monitored by fluorescence microscopy in cells infected with wild-type (wt) and ts mutants as well as M1 gene transfected cells. The results suggest that the $\mu 2$ protein plays a crucial role in the formation of reovirus inclusions, perhaps by influencing the rate of biochemical events or by forming a structural lattice for inclusion formation.

RESULTS

Reovirus exhibits strain-specific differences in the rate of inclusion formation in L929 cells

To determine whether T1L and T3D differ in kinetics of inclusion formation in L929 cells, we used indirect immunofluorescence to assess the relative proportion of antigen-positive cells that formed cytoplasmic inclusions. Cells were infected with either T1L or T3D at a multiplicity of infection (m.o.i.) of 10 plaque-forming units (PFU) per cell. The cells were then fixed in acetone at varying times after infection and stained with strain-specific rabbit antisera followed by donkey anti-rabbit antiserum conjugated to Cy3. Viral inclusions were seen as local concentrated areas of staining within the cytoplasm relative to generalized cytoplasmic staining (Fig. 1A, thin and heavy arrows, respectively). Cells showing intermediate staining patterns were scored as inclusion-negative. Immunofluorescence staining showed that viral antigen was diffusely distributed in the cytoplasm in the majority of T1L-infected cells at 12 and 24 h postinfection (p.i.) but was seen to localize into inclusions by 48 h p.i. (Figs. 1A and 1C and Table 1). In contrast,

TABLE 1

Rate of Inclusion Formation in T1L- or T3D-Infected L929 Cells		
Time postinfection (hours)	Percentage inclusions ^a	
	T1L (<i>n</i>) ^b	T3D (<i>n</i>)
15	4 ± 2 (328)	46 ± 2 (35)
20	7 ± 8 (79)	67 ± 15 (37)
24	11 ± 9 (219)	66 ± 4 (84)
48	63 ± 10 (251)	nd

^a Average of two to three experiments.

^b *n* is the number of antigen-positive cells counted; nd, not done.

inclusion formation in T3D-infected cells was observed at much earlier time points, with a majority of cells showing inclusions by 20 h p.i. (Figs. 1B and 1D and Table 1). T1L and T3D differed strikingly in the rate of inclusion formation with median times of 39 and 18 h, respectively. These results demonstrate that reovirus strains T1L and T3D differ in the rate of inclusion formation in L929 cells.

Strain-specific differences in the rate of reovirus inclusion formation are determined primarily by the M1 gene

To identify viral genes that segregate with differences in the kinetics of inclusion formation exhibited by T1L and T3D, we tested 15 T1L × T3D reassortant viruses for the rate of inclusion formation in L929 cells by immunofluorescence staining at 24 h p.i. (Table 2). This time point was chosen because it demonstrated a maximum

difference in the extent of inclusion formation by T1L- and T3D-infected L929 cells (Table 1). Those reassortant viruses that produced the greatest percentage of infected cells with inclusions at 24 h p.i. possessed a T3D M1 gene, while those that produced the least contained a T1L M1 gene. Reassortant viruses containing a T3D M1 gene and a T1L S3 gene produced inclusions with faster kinetics than the T3D parent. The rate of inclusion formation of reassortant viruses containing a T1L M1 gene was, however, not influenced by the allelic nature of the S3 gene. The association of the M1 gene with the rate of inclusion formation was highly statistically significant (*t* test, $P < 0.0001$; Mann-Whitney (MW) test, $P < 0.001$). The remaining genes were not significantly associated with the rate of inclusion formation in these experiments (*t* test and MW test, $P > 0.05$). We used parametric stepwise linear regression analysis to determine the individual contribution of genes to the rate of inclusion formation. This analysis showed that 89.8% ($P = 0.027$) of the variability in inclusion formation is accounted for by the 10 reovirus genes with 86% contributed by the M1 gene ($P < 0.001$), 7% by the S3 gene ($P = 0.169$), and 4% by the S1 gene ($P = 0.649$). There was no detectable contribution by the other viral genes to this phenotypic difference. These results indicate that M1 is the only viral gene that independently contributes to the rate of reovirus inclusion formation. When only those reassortant viruses containing a T3D M1 gene ($n = 10$) were analyzed, the S3 gene was the only gene significantly associated with the rate of inclusion formation (*t* test, $P = 0.004$; MW test, $P = 0.014$). These results indicate that the rate of viral inclusion formation is

TABLE 2

Inclusion Formation in L929 Cells Exhibited by T1L × T3D Reassortant Viruses

Virus strain	Parental origin of gene segments										Percentage inclusion formation (<i>n</i>) ^a	Rank
	L1	L2	L3	M1	M2	M3	S1	S2	S3	S4		
EB129	3	3	3	3	3	1	3	1	1	3	96.2 (157)	1
G16	1	1	1	3	1	1	1	3	1	1	88.4 (69)	2
EB123	3	3	1	3	3	3	3	3	1	3	79.4 (160)	3
EB146	1	1	1	3	1	1	1	1	1	3	76.3 (97)	4
EB88	3	3	3	3	1	3	3	3	3	3	65.6 (162)	5
T3D	3	3	3	3	3	3	3	3	3	3	65.5 (84)	6
EB96	1	3	1	3	1	1	1	1	3	1	64.8 (88)	7
EB28	3	3	1	3	3	3	3	1	3	3	64.1 (167)	8
EB86	1	3	3	3	3	1	3	3	3	1	46.0 (174)	9
EB31	1	1	1	3	1	1	1	3	3	1	38.2 (110)	10
H60	3	3	1	1	3	3	3	3	3	1	29.6 (81)	11
H15	1	3	3	1	3	3	3	3	3	1	27.0 (89)	12
EB39	1	3	3	1	3	3	3	3	3	3	19.3 (88)	13
EB47	1	3	1	1	1	1	1	1	1	1	14.5 (124)	14
T1L	1	1	1	1	1	1	1	1	1	1	11.0 (219)	15
H17	3	3	1	1	3	3	1	3	3	1	7.6 (92)	16
EB73.1	1	3	1	1	3	3	3	3	3	3	6.5 (124)	17

^a *n* is the total number of antigen-positive cells counted by immunofluorescence staining with rabbit polyclonal anti-T1L and -T3D antisera.

due primarily to the M1 gene, which encodes the $\mu 2$ protein, and is modulated by the S3 gene, which encodes the nonstructural protein σ NS.

Colocalization of $\mu 2$ and other reovirus proteins in cytoplasmic inclusions

The observation that the M1 gene is the primary determinant of strain-specific differences in the rate of viral inclusion formation led us to examine the subcellular localization of $\mu 2$ protein with respect to other reovirus proteins during infection of L929 cells. A monoclonal antibody (8H6) specific for $\mu 1/\mu 1C$ (Virgin *et al.*, 1991), a reovirus outer-capsid protein, was used to identify reovirus inclusion bodies, and rabbit anti-T1L- $\mu 2$ polyclonal antiserum was used to detect $\mu 2$ protein. The polyclonal rabbit anti-T1L- $\mu 2$ antiserum demonstrated equivalent reactivity with both T1L and T3D $\mu 2$ proteins, which are 98.6% identical in amino acid sequence, by both immunoprecipitation (Zou and Brown, 1996b) and immunoblot (data not shown). To determine the subcellular distribution of $\mu 2$ relative to other reovirus proteins during infection, double-immunofluorescence labeling of cells infected with either T1L or T3D was performed using confocal laser scanning microscopy. T3D $\mu 2$ protein was primarily concentrated in inclusions, whereas T1L $\mu 2$ protein had a more diffuse distribution (Figs. 2E and 2F). However, in cells infected with either strain, $\mu 2$ and $\mu 1/\mu 1C$ proteins colocalized in cytoplasmic inclusions (Figs. 2E, 2F, 2H, 2I, 2K, and 2L). In addition, $\mu 2$ protein localized to the nucleus in both T3D- and T1L-infected cells (Figs. 2E and 2F). The presence of the $\mu 2$ protein in the nucleus was confirmed by costaining with a dsDNA-specific dye, ToPro3 (Figs. 2K and 2L). Occasionally, $\mu 2$ protein was observed to accumulate in small cytoplasmic foci that were not associated with $\mu 1/\mu 1C$ staining (Fig. 2L). These results indicate that $\mu 2$ localizes to sites of viral assembly and is also distributed in the nucleus.

$\mu 2$ protein localization in cells infected with reovirus temperature-sensitive mutants

We used temperature-sensitive mutants that are defective in viral assembly to further examine the role of $\mu 2$ protein in inclusion formation. The temperature-sensitive mutant tsH11.2 does not replicate at nonpermissive temperature (39.5°C) due to a conditionally defective $\mu 2$ protein (Coombs, 1996). Progeny virions are not observed in tsH11.2-infected cells due to a defect in viral assembly and genome replication. Infection of L929 cells with tsH11.2 at a permissive temperature (33°C) resulted in normal inclusions with colocalization of $\mu 2$ and $\mu 1/\mu 1C$ proteins (data not shown). Infection of L929 cells with tsH11.2 at a nonpermissive temperature resulted in the accumulation of $\mu 1/\mu 1C$ protein in subcellular structures that did not contain $\mu 2$ protein and were generally smaller than inclusions observed in cells infected with

wild-type virus (Figs. 3G and 3J). Instead, $\mu 2$ protein had a diffuse cytoplasmic and nuclear localization (Figs. 3D and 3I). These results demonstrate that subcellular structures that resemble inclusions by phase-contrast microscopy can form without $\mu 2$ protein as in wt infection. To determine whether viral inclusion formation was affected by defects in other viral genes, two other ts mutants, tsC447 and tsG453, with mutations in the $\sigma 2$ -encoding S2 and $\sigma 3$ -encoding S4 genes, respectively, were used to infect L929 cells. Infection with either ts mutant resulted in the accumulation of $\mu 1/\mu 1C$ protein in subcellular structures that did not stain for $\mu 2$ protein (Figs. 3H, 3I, 3K, and 3L). In contrast to tsH11.2, infection with tsC447 and tsG453 resulted in the accumulation of $\mu 2$ in small protein complexes seen as punctate cytoplasmic staining adjacent to subcellular structures containing $\mu 1/\mu 1C$ protein, in addition to having diffuse nuclear staining (Figs. 3E, 3F, 3K, and 3L). Occasionally, $\mu 2$ protein was also seen to accumulate in discrete structures in the nucleus (Fig. 3F).

Recombinant T1L and T3D $\mu 2$ proteins form nuclear and cytoplasmic complexes at different rates

Genetic analysis of the rate of reovirus inclusion formation indicated that this property is linked to the $\mu 2$ -encoding M1 gene. Accumulation of $\mu 2$ in protein complexes independent of $\mu 1/\mu 1C$ protein also was observed in cells infected with either wt viruses or ts mutants (Figs. 2L, 3K, and 3L). These observations suggested that $\mu 2$ would be capable of forming protein complexes in cells independent of other viral proteins. To examine this possibility, recombinant $\mu 2$ protein was expressed in L929 cells by transfection with either T1L or T3D M1 gene-containing plasmids under control of a bacteriophage T7 RNA polymerase promoter. Immunoblot analysis of transfected cells showed high levels of $\mu 2$ protein expression 24 h posttransfection for both the T1L and the T3D M1 gene constructs (Fig. 4). In contrast, expression of T1L $\mu 2$ was more robust than T3D $\mu 2$, in cells infected with these virus strains (Fig. 4). M1-gene transfected cells were stained for $\mu 2$ protein at 24 and 48 h after transfection. The $\mu 2$ protein of both T1L and T3D formed complexes in the absence of the other reovirus proteins (Figs. 5C, 5D, 5E, and 5F). The rate of complex formation varied in a strain-specific manner. The median time of complex formation by T3D $\mu 2$ protein was 22 h posttransfection compared to 43 h posttransfection for cells expressing T1L $\mu 2$ protein (Table 3; Figs. 5B, 5C, 5D, and 5E). Differences in the rate of complex formation exhibited by T1L and T3D $\mu 2$ proteins paralleled that of inclusion formation in reovirus-infected cells. Recombinant $\mu 2$ protein formed complexes in both the nucleus and the cytoplasm (Fig. 5D). The presence of nuclear $\mu 2$ complexes was confirmed using confocal laser scanning microscopy and dual staining for $\mu 2$ and

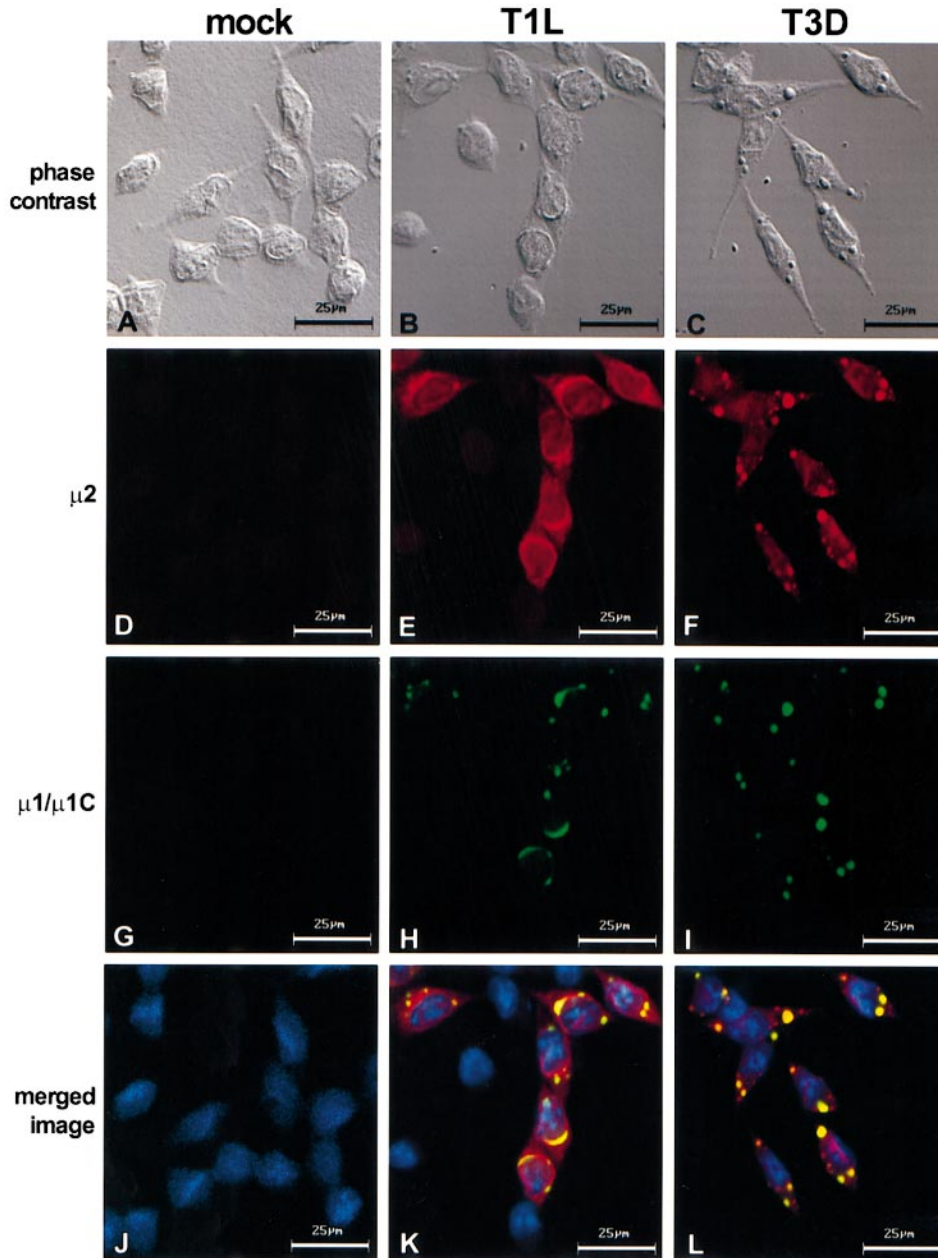


FIG. 2. Subcellular localization of reovirus $\mu 2$ and $\mu 1/\mu 1C$ proteins in cells infected with reovirus strains T1L or T3D. L929 cells were either mock-infected (A, D, G, J) or infected with T1L (B, E, H, K) or T3D (C, F, I, L) at an m.o.i. of 10 PFU per cell. Following adsorption, cells were incubated at 37°C for 18 h. Cells were stained for $\mu 2$ using a $\mu 2$ -specific polyclonal antiserum (D–F) and for $\mu 1/\mu 1C$ using $\mu 1/\mu 1C$ -specific mAb 8H6 (G–I) as primary antibodies followed by goat anti-mouse Alexa488 and goat anti-rabbit Alexa546 as secondary antibodies. The $\mu 2$ protein is colored red, and the $\mu 1/\mu 1C$ protein is colored green. ToPro3, a dsDNA-specific dye, was incubated with the secondary antibodies and is colored blue (J–L). Images were obtained using a confocal laser scanning microscope. A phase-contrast image of each field is shown in A–C. In the merged images, colocalization of $\mu 2$ and $\mu 1/\mu 1C$ is indicated by the yellow color, and colocalization of $\mu 2$ and ToPro3 is indicated by the pink color.

the nucleus (data not shown). Expression of recombinant tsH11.2 $\mu 2$ protein resulted in temperature-sensitive complex formation at permissive relative to nonpermissive temperature at 48 h posttransfection ($17 \pm 9\%$ vs $7 \pm 7\%$ of antigen-positive cells; *t* test, $P = 0.047$). However, the number of cells containing $\mu 2$ complexes after transfection with tsH11.2 $\mu 2$ at both permissive and nonpermissive temperatures was significantly less than

that after transfection with wt T1L $\mu 2$ protein ($17 \pm 9\%$ and $7 \pm 7\%$ vs $56 \pm 8\%$ for T1L $\mu 2$; *t* test, $P < 0.00001$). The expression level of recombinant tsH11.2 $\mu 2$ protein was comparable to that of wt T1L (data not shown). This finding suggests that the M1 mutation in tsH11.2 impairs the capacity of tsH11.2 $\mu 2$ to form protein complexes when expressed on its own.

To further assess the localization of recombinant $\mu 2$

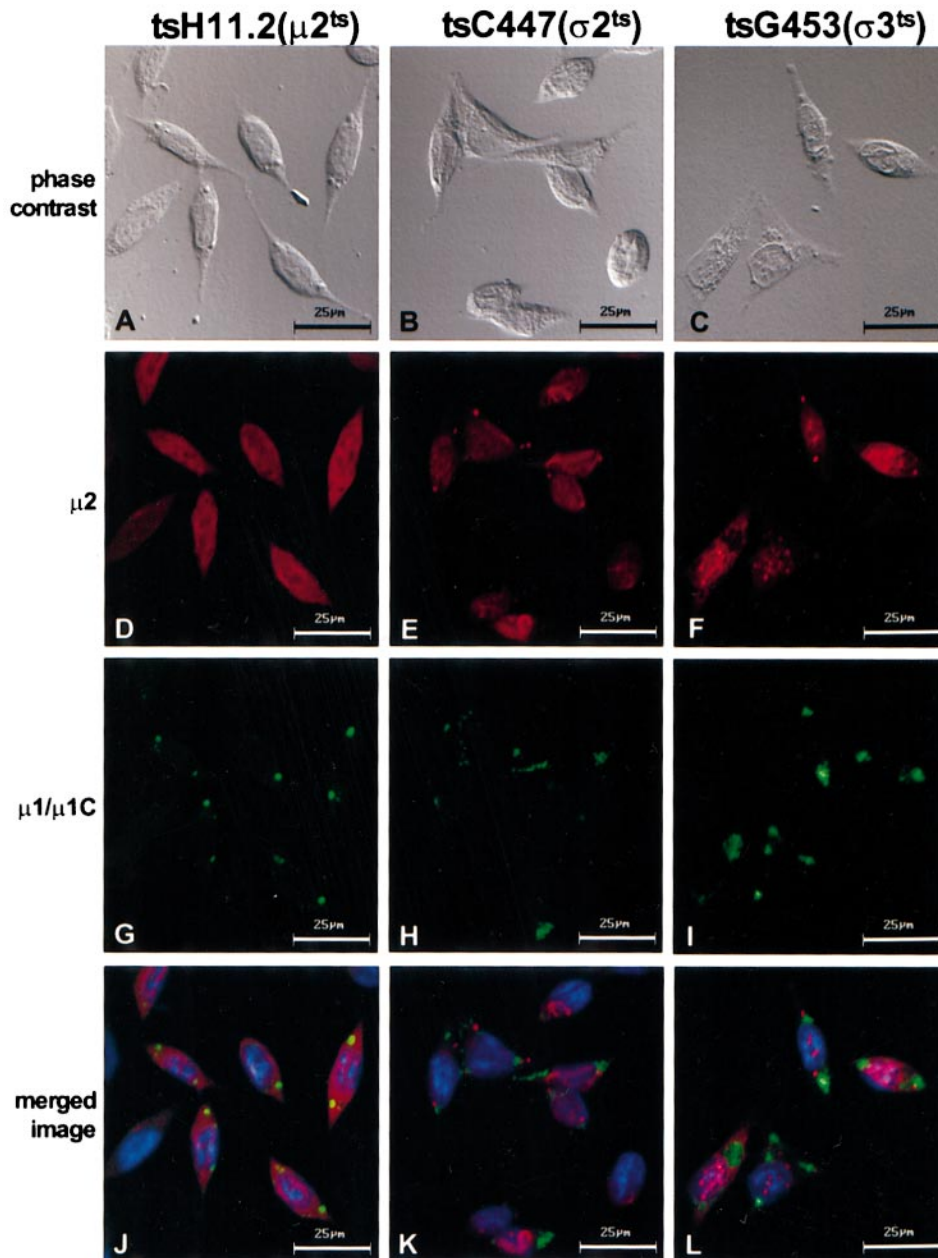


FIG. 3. Subcellular localization of reovirus $\mu 2$ and $\mu 1/\mu 1C$ proteins in cells infected with ts mutant reoviruses tsH11.2, tsC447, and tsG453. L929 cells were infected with either tsH11.2 (A, D, G, J), tsC447 (B, E, H, K), or tsG453 (C, F, I, L) at an m.o.i. of 10 PFU per cell. Following adsorption, cells were incubated at 39.5°C for either 24 h (tsH11.2 and tsC447) or 36 h (tsG453). Cells were stained for $\mu 2$ using a $\mu 2$ -specific polyclonal antiserum (D–F) and for $\mu 1/\mu 1C$ using $\mu 1/\mu 1C$ -specific mAb 8H6 (G–I) as primary antibodies followed by goat anti-mouse Alexa488 and goat anti-rabbit Alexa546 as secondary antibodies. The $\mu 2$ protein is colored red, and the $\mu 1/\mu 1C$ protein is colored green. ToPro3, a dsDNA-specific dye, was incubated with the secondary antibodies and is colored blue (J–L). Images were obtained using a confocal laser scanning microscope. A phase-contrast image of each field is shown in A–C. In the merged images, colocalization of $\mu 2$ and $\mu 1/\mu 1C$ is indicated by the yellow color, and colocalization of $\mu 2$ and ToPro3 is indicated by the pink color.

protein, transfected cells were fractionated into soluble (cytoplasmic) and pellet (nuclear) fractions by detergent extraction and sedimentation. The resulting samples were analyzed by immunoblot using a T1L $\mu 2$ -specific antiserum. Both T1L and T3D $\mu 2$ proteins were found in the soluble and pellet fractions (Fig. 6). Quantification by phosphorimaging showed that 61% of the T3D $\mu 2$ protein compared to 49% of the T1L $\mu 2$ protein had accumulated

in the pellet by 24 h posttransfection. This observation is consistent with the nuclear localization of T3D and T1L $\mu 2$ proteins as seen by immunofluorescence. The integrity of the fractionation procedure was verified by staining the same samples for tubulin, a cytoplasmic protein, which was present only in the soluble fraction (Fig. 6). These data support the nuclear localization of $\mu 2$ protein observed in reovirus-infected cells.

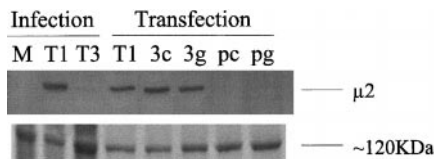


FIG. 4. Immunoblot analysis of $\mu 2$ protein expression in infected and transfected L929 cells. Cell lysates were collected 24 h p.i. or post-transfection, and the blot was probed with anti-T1L- $\mu 2$ antiserum. Lane annotation from left to right: Infection: M, mock-infected; T1, T1L-infected; T3, T3D-infected. Transfection: T1, pCMV-M1CN T1-7; 3c, pCMV-M1CN T3-13; 3g, pGEM-M1 T3-18; pc, pcDNA3 vector control; and pg, pGEM7 vector control transfected. (Bottom) The same samples stained with Coomassie blue showing a protein of approximately 120 kDa, as a loading control.

DISCUSSION

In this study, we show that reovirus strains T1L and T3D differed in the rate of inclusion formation in L929 cells. This finding is consistent with early studies of the rate of inclusion formation by T1L (Rhim *et al.*, 1962) and T3D (Gomatos *et al.*, 1962). Genetic analysis using T1L \times T3D reassortant viruses showed that the M1 gene is the primary determinant of strain-specific differences in the kinetics of inclusion formation. Since T1L synthesizes several-fold more $\mu 2$ protein and other reovirus proteins than T3D (Fig. 4; Mbisa and Brown, unpublished data;

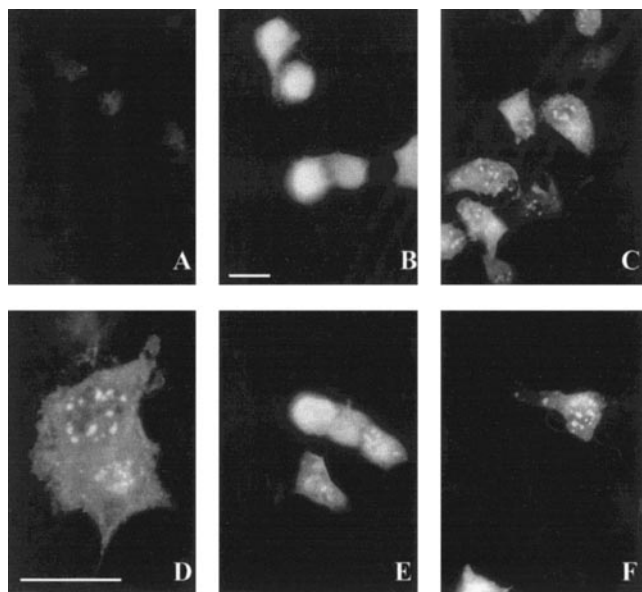


FIG. 5. Localization of recombinant $\mu 2$ protein in transfected cells. L929 cells were transfected with control vector (pcDNA3) (A), pCMV-M1CN clone T1-7 expressing the T1L M1 gene (B, E), or transfected with pCMV-M1CN clone T3-13 expressing the T3D M1 gene (C, F). Following incubation for either 24 h (A, B, C) or 48 h (E, F), cells were stained for $\mu 2$ using $\mu 2$ -specific rabbit polyclonal antiserum followed by FITC-conjugated goat anti-rabbit antiserum. (D) Higher magnification of cells transfected with pGEM-M1 clone T3-18 expressing the T3D M1 gene, stained for $\mu 2$ at 24 h posttransfection showing nuclear and cytoplasmic complexes of $\mu 2$. The bars represent 10 μ m.

TABLE 3

Rate of $\mu 2$ Complex Formation in L929 Cells Transfected with the T1L or T3D M1 cDNA

Time posttransfection (hours)	Percentage cells with protein complex formation ^a	
	T1L M1 cDNA (n) ^b	T3D M1 cDNA (n)
24	15 \pm 10 (132)	61 \pm 11 (88)
48	56 \pm 8 (115)	98 \pm 5 (26)

^a Average of two to four experiments (at least one with pGEM and pcDNA3).

^b n is the number of antigen-positive cells counted by immunofluorescence staining with rabbit polyclonal anti-T1L $\mu 2$ antiserum.

Schmechel *et al.*, 1997; Matoba *et al.*, 1991) and yet forms inclusions at a slower rate, it is likely that an intrinsic difference in T1L and T3D $\mu 2$ proteins influences the rate of inclusion formation in reovirus-infected cells.

The S3 gene modulated the rate of inclusion formation in conjunction with the M1 gene such that pairing of a T1L S3 gene with a T3D M1 gene in T1L \times T3D reassortant viruses resulted in a faster rate of inclusion formation than for the parental strain T3D. This finding indicates that the T3D S3 gene attenuates the rate of inclusion formation by the cognate T3D M1 gene. The strain of origin of the S3 gene did not affect the kinetics of inclusion formation when paired with the T1L M1 gene, indicating that the T1L $\mu 2$ protein differs from T3D $\mu 2$ in its interactions with σ NS. It is possible that the σ NS protein modulates the rate of inclusion formation by direct interactions with $\mu 2$.

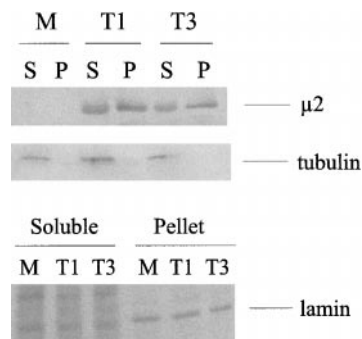


FIG. 6. Immunoblot analysis of recombinant $\mu 2$ protein in the soluble (cytoplasmic) and pellet (nuclear) fractions of cells transfected with either the T1L or the T3D M1 gene. Cell lysates were collected and fractionated at 24 h posttransfection, and the blot was probed with polyclonal rabbit anti-T1L- $\mu 2$ antiserum and detected by phosphorimaging. The middle panel shows an immunoblot of the same samples stained for tubulin, a cytoplasmic protein that is present only in the soluble fraction. (Bottom) The same samples stained with Coomassie blue showing a protein in the pellet fractions of 67 kDa corresponding to lamin and unidentified proteins in the soluble fractions as loading controls. M, mock transfected; S, soluble fraction; P, pellet fraction; T1, T1L M1 gene transfected; T3, T3D M1 gene transfected.

In addition to controlling the rate of inclusion formation, the $\mu 2$ protein might play a direct physical role in the inclusion formation process. This hypothesis is supported by expression of recombinant $\mu 2$ protein in L929 cells, which resulted in the formation of protein complexes that resemble inclusions. Although these $\mu 2$ complexes were not associated with other viral proteins or the host protein vimentin (Mbisa and Brown, unpublished data), they were formed with kinetics that reflect the parental origin of the M1 gene. However, $\mu 2$ protein is probably not the only reovirus protein involved in inclusion formation. Infection of L929 cells with mutants tsH11.2, tsC447, and tsG453 resulted in the formation of subcellular structures that resembled reovirus inclusions but did not contain $\mu 2$ protein. In addition, at least one other reovirus protein, $\mu 1/\mu 1C$, has been shown to form protein complexes when expressed alone (Yue and Shatkin, 1996). The $\sigma 1$ protein also has been shown to have a uniform cytoplasmic distribution or to accumulate in punctate foci in different studies using different cell lines for transfection (Banerjee *et al.*, 1988; Belli and Samuel, 1991). Inclusion formation may thus be a concerted function of several reovirus proteins with $\mu 2$ protein controlling the formation rate. Alternatively, $\mu 2$ could coordinate the formation of a subset of protein complexes that serve as a prerequisite for inclusion formation.

In addition to localizing to cytoplasmic inclusions, $\mu 2$ localizes to the nucleus in cells infected with wt reovirus, in cells infected with mutant viruses tsH11.2, tsC447, and tsG453, and in M1-gene-transfected cells. The localization of the protein to the nucleus was unanticipated, considering that reovirus replication is thought to be entirely cytoplasmic. It is possible that $\mu 2$ protein localizes to the nucleus to induce cellular events involved in reovirus replication, including inclusion formation. Both recombinant T1L and T3D $\mu 2$ proteins accumulate in the nucleus to similar levels in transfected cells, although T3D $\mu 2$ protein produced complexes more rapidly than T1L $\mu 2$ protein. This observation may be relevant to the inclusion formation process since the activity parallels the rate of inclusion formation during infection. The $\mu 2$ protein is not the only reovirus protein that localizes to the nucleus. The $\sigma 3$ protein accumulates in the nucleus of both infected and transfected cells (Yue and Shatkin, 1996; Schmechel *et al.*, 1997), and $\sigma 1s$, a nonstructural protein encoded by the S1 gene, localizes to the nucleus (Belli and Samuel, 1991; Rodgers *et al.*, 1998).

Sequence analysis of the $\mu 2$ protein reveals a prototypical nuclear localization signal motif at positions 261 to 264 (KRLR) that fits a consensus sequence, K R/K X R/K (Garcia-Bustos *et al.*, 1991; Mukaigawa and Nayak, 1991), required for the nuclear localization of several proteins including the PB1 and PB2 subunits of the influenza virus RNA polymerase (Nath and Nayak, 1990; Mukaigawa and Nayak, 1991). Nuclear localization signals have also been shown to consist of a single stretch

of basic amino acids (Chelsky *et al.*, 1989; Garcia-Bustos *et al.*, 1991) and one such region is present in the $\mu 2$ protein from position 100 to 114 (RRLRKRLMLKKDLRK). Experiments are in progress to identify sequences in the M1 gene required for nuclear localization and complex formation of the $\mu 2$ protein.

The $\mu 2$ protein did not accumulate in protein complexes in cells infected at nonpermissive temperature with tsH11.2, and although complexes were observed in cells expressing high levels of recombinant tsH11.2 $\mu 2$ protein they were formed less efficiently, even at permissive temperatures, than wt T1L $\mu 2$ protein. These findings suggest that the mutations in the tsH11.2 $\mu 2$ protein affect the accumulation of $\mu 2$ in complexes. The tsH11.2 M1 gene has two mutations resulting in 2 amino acid substitutions that are 11 residues apart, M³⁹⁹ \rightarrow T and P⁴¹⁴ \rightarrow H (Coombs, 1996). Constitutive expression of wt $\mu 2$ protein in L929 cells complements the M1 defect of tsH11.2 at nonpermissive temperatures (Zou and Brown, 1996a). Expression of $\mu 2$ proteins containing either single mutation is capable of partially complementing the tsH11.2 defect, which indicates that both mutations contribute to the ts phenotype (Zou, Brown, and Coombs unpublished results; Coombs, 1998b). The P⁴¹⁴ \rightarrow H mutation resides in a region with partial homology to the A motif of known ATPases (Noble and Nibert, 1997). This observation raises the possibility that $\mu 2$ protein mediates the rate of inclusion formation directly by an ATP- or other nucleotide-dependent event or indirectly through an ATP-dependent interaction with host regulatory proteins. Consistent with this idea, the M1 gene, in addition to the L3 gene, influences the NTPase activity of reovirus cores (Noble and Nibert, 1997).

Reovirus assembly is poorly understood, but the earliest ssRNA-containing structures termed "assortment" complexes are composed of σNS , μNS , $\sigma 3$, $\mu 1/\mu 1C$, $\lambda 1$, and $\lambda 2$ (Antczak and Joklik, 1992). Progeny, core-like, subviral particles also acquire three other proteins that are not found in assortment complexes; $\mu 2$, $\lambda 3$, and $\sigma 2$. This results in the formation of replicase particles containing all the viral structural proteins as well as μNS (Zweerink *et al.*, 1976). These particles are transcriptionally active progeny subviral particles and synthesize dsRNA. It is possible that ssRNA-containing complexes associate with another complex containing $\mu 2$, $\lambda 3$, and $\sigma 2$ and that the $\mu 2$ protein controls the formation of this complex at the site of inclusion formation. Since the M1 gene determines the rate of inclusion information, the formation of this complex could be the rate-limiting step. The secondary role of the S3 gene in kinetics of inclusion formation suggests that σNS influences the rate of formation of the ssRNA-containing complex. Alternatively, σNS might directly interact with $\mu 2$ to form replicase particles. Such an association could be modulated by the different M1 and S3 genes to affect the rate of inclusion formation. This model predicts that the $\mu 2$ protein does

not associate with $\mu 1/\mu 1C$ -containing complexes in either tsC447- or tsG453-infected cells that express mutant $\sigma 2$ and $\sigma 3$ proteins, respectively. The absence of $\mu 2$ in $\mu 1/\mu 1C$ -containing complexes in cells infected with these ts mutants would result from failure of the $\mu 2$ protein to recognize the aberrant structures produced during these infections due to mutations in $\sigma 2$ and $\sigma 3$. Our future experiments will address the interactions of individual viral proteins in wt and ts reovirus infections to clarify the sequence of events leading to inclusion formation. Nonetheless it is interesting that the only reovirus ts mutants that are completely defective in virion assembly—where capsid structures do not form—are tsH (M1 gene) and tsE (S3 gene) (reviewed by Coombs, 1998b), which supports the hypothesis that virion assembly and inclusion formation are functionally linked and that $\mu 2$ and σNS play crucial roles in both of these processes.

Host tissue-dependent effects of reovirus infection that segregate with the M1 gene may be explained in part by the differential capacity of the $\mu 2$ protein to influence the rate of inclusion formation. This $\mu 2$ -mediated property might in turn be dependent on the capacity of the $\mu 2$ protein to interact with host factors and form inclusions, which are indicative of successful viral assembly. Identification of host constituents associated with viral inclusions in reovirus-infected cells should provide insight into mechanisms of reovirus genome replication and assortment. Knowledge of the inclusion formation process, including identification of the protein–protein and protein–RNA interactions required for inclusion formation, will contribute to an understanding of viral assembly and identify new therapeutic targets for dsRNA-containing viruses.

MATERIALS AND METHODS

Cells and viruses

Mouse fibroblast L929 cells were propagated in adherent culture in MEM (Gibco BRL, Burlington, Ontario, Canada) supplemented to contain 5% fetal calf serum (Biocell Laboratories, Carson, CA). Reovirus strains T1L and T3D were laboratory stocks initially obtained from Dr. B. N. Fields. The ts mutants tsC447, tsG453, and tsH11.2 were provided by Dr. K. Coombs (University of Manitoba). The T1L \times T3D reassortant viruses were produced previously (Brown *et al.*, 1983). The recombinant vaccinia virus vTF7.3 that expresses the T7 RNA polymerase was a kind gift from Dr. K. Dimock (University of Ottawa) and was grown in CV-1 cells. Reoviruses were propagated and titrated by plaque assay in L929 cells as described previously (Zou and Brown, 1992).

Antibodies

Antisera to T1L and T3D $\mu 2$ proteins were produced in rabbits immunized with Trp-E- $\mu 2$ fusion protein ex-

pressed in *Escherichia coli* (Zou and Brown, 1996a). Antisera to reovirus strains T1L and T3D were generated by immunizing rabbits with purified reovirus. Prior to use in indirect immunocytochemistry the antisera were adsorbed to acetone-fixed L929 cell extract and used at a dilution of 1 in 500. Monoclonal antibody 8H6, specific for $\mu 1/\mu 1C$ protein, was used at a concentration of 10 $\mu g/ml$ to detect reovirus inclusions in dual-labeling experiments. The primary antibody used to detect cytoskeletal proteins was murine monoclonal antibody against β -tubulin (Clone DM1B, Amersham, Baie d'Urfe, Quebec, Canada; at 1:1000).

Secondary antibodies used were fluorescein-conjugated goat anti-rabbit IgG (Sigma Chemical Co., Oakville, Ontario, Canada) and Cy3-conjugated donkey anti-rabbit (Jackson ImmunoResearch Laboratories, Inc., West Grove, PA). Goat anti-mouse Alexa488 and goat anti-rabbit Alexa546 (Molecular Probes, Inc., Eugene, OR) were used in dual-labeling experiments at a dilution of 1:1000. ToPro3, a dsDNA-specific dye (Molecular Probes), was used to detect the nucleus at a dilution of 1:1000. Protein A conjugated to alkaline phosphatase and anti-mouse IgG conjugated to alkaline phosphatase were obtained from Sigma Chemical Co.

Indirect immunostaining

L929 cells seeded on 22 \times 22 mm glass coverslips (Corning Inc., Big Flats, NY) in 6-well plates were infected with reovirus strains T1L or T3D at a m.o.i. of 10 PFU per cell. Prior to being stained, the cells were fixed in pre-chilled acetone for 5 min. After being rinsed in PBS (3 \times 5 min), 100 μl of an appropriate dilution of antisera was applied and incubated in a humidified chamber at room temperature for 30–90 min. The coverslips were then rinsed in PBS (3 \times 5 min) and treated with the appropriate dilution of the secondary conjugated antibody. After another 30- to 90-min incubation period at room temperature the coverslips were rinsed in PBS (3 \times 5 min) and once in ddH₂O and mounted on glass slides in Gel/Mount (Biomedica Corp). All antibody dilutions were done in PBS/3% BSA. Mock infections were done and analyzed for every experiment as a negative control. The samples were visualized using a Zeiss microscope equipped with epifluorescence and a 63X or 100X, 1.40 NA PlanApo objective. The images were collected using Image One Metamorph software (Universal Imaging Corp., West Chester, PA) and a Hamamatsu chilled charge-coupled digital camera (Model C5985, Hamamatsu Corp., Bridgewater, NJ).

For double-immunolabeling the cells were fixed for 2 min in a 1:1 (v/v) mixture of methanol and acetone. Cells were kept in methanol at $-20^{\circ}C$ until stained. Cells were then washed twice in PBS and incubated for 15 min in PBS containing 5% BSA (Sigma, St. Louis, MO). Nonspecific binding of antibody to cells was blocked by incuba-

tion for 10 min in PBS containing 1% BSA, 1% Triton X-100 (Bio-Rad Laboratories, Hercules, CA), and 2% normal goat serum (Vector Laboratories, Inc., Burlingame, CA). All washes and antibody dilutions were done in the same solution. Cells were then incubated with primary and secondary antibodies and ToPro3 as described above. Cells were washed twice for 15 min with PBS/1% BSA, 1% Triton X-100 and then twice for 10 min with PBS. Coverslips were washed with deionized water and then mounted on glass slides using ProLong Antifade (Molecular Probes). Cells were visualized using a Zeiss confocal fluorescence microscope (Carl Zeiss, New York, NY), and the images were processed and colored using Adobe Photoshop (Adobe Systems, Inc., San Jose, CA).

Transfection

L929 cells seeded in 6-well plates containing 22×22 mm glass coverslips (Corning) were transfected with DNA using lipofectin reagent when they were at 80–85% confluence using the protocol from Gibco BRL. Five micrograms of DNA and 15 μ l of lipofectin were used for each transfection reaction. M1 DNA constructs pCMV-M1CN (clones T1-7 and T3-13) and pGEM-M1 (clones T1-7 and T3-18) both under control of the bacteriophage T7 promoter were used (Zou and Brown, 1996b). After a 5-h incubation period the cells were infected with the recombinant vaccinia vTF7.3 at an m.o.i. of 0.5 to 1. The cells were then incubated for 24 or 48 h at 37°C before analysis.

Immunoblotting

Infected or transfected cell monolayers were lysed in SDS sample buffer (62.5 mM Tris-HCl, pH 6.8, 10% glycerol, 2% SDS, 0.05% bromophenol blue, and 5% 2-mercaptoethanol). The proteins were separated by SDS-PAGE and transblotted onto Immobilon P membrane (Millipore, Mississauga, Ontario, Canada) at 25 V overnight at 4°C. The dried membrane was blocked with 5% skim milk in PBS for 1 h at RT. This was followed by the addition of primary antibody in fresh milk and incubation for 2 h at 4°C. The membrane was then washed three times in PBS and once in TBS to remove phosphate and incubated in 5% milk in TBS containing 1 μ g/ml PAAP. Finally the membrane was washed 4 \times in TBS before reaction with chromogenic substrate, nitro blue tetrazolium (33 μ l/ml) plus 5-bromo-4-chloro-3-indolyl phosphate (3.3 μ l/ml) (Sigma), in alkaline phosphatase buffer (100 mM NaCl, 5 mM MgCl₂, and 100 mM Tris-HCl, pH 9.5) or Attophos reagent (JBL Scientific, San Luis Obispo, CA) for phosphorimaging using a Storm 860 PhosphorImager equipped with ImageQuant software (Molecular Dynamics). For quantification purposes known amounts of TrpE- μ 2 fusion protein were run as reference and only μ 2 protein readings falling within the linear range of the reference were considered significant.

Cell fractionation

Adherent transfected cells were washed with cold PBS, lysed in lysis buffer (10 mM PIPES, pH 6.8, 100 mM NaCl, 300 mM sucrose, 3 mM MgCl₂, 1 mM EGTA, 4 mM vanadyl riboside complex, 0.5% (v/v) Triton X-100, and 1.2 mM PMSF), and scraped into a microfuge tube (He *et al.*, 1990). To collect the cytoplasmic and nuclear fractions, a modification of the procedure described by He *et al.* (1990) was used. Briefly, the samples were centrifuged (600 *g* for 3 min), the supernatant was decanted (cytoplasmic fraction), and the pellet was then rinsed with RSB buffer (10 mM Tris, pH 7.4, 10 mM NaCl, 1.5 mM MgCl₂, and 1 mM PMSF) and resuspended in 1 \times sample buffer (nuclear fraction). The samples were then resolved by SDS-PAGE and electroblotted to a PVDF membrane before immunoblotting as described above.

Statistical analysis

The association of reovirus gene segments with the rate of inclusion formation was determined by using *t* test (parametric) and MW test (nonparametric) statistical techniques. The contributions of individual genes were analyzed further by parametric stepwise linear regression and additional linear regression analysis was performed for all combinations of genes found to be statistically significant. Statistical analyses were performed by using the Minitab (release 8) statistical software package (Addison-Wesley, Reading, MA).

ACKNOWLEDGMENTS

We thank Ken Tyler for assistance with statistical analysis of the reassortant data. Useful criticism of the manuscript was provided by B. Sherry, K. Coombs, and N. Chaly. This work was supported by NSERC Canada Grant OGP0041771 (E.G.B.), Public Health Service Award A132539 from the National Institute of Allergy and Infectious Diseases (T.S.D.), and the Elizabeth B. Lamb Center for Pediatric Research (M.M.B. and T.S.D.). Additional support was provided by Public Health Service Awards DK20593 for the Vanderbilt Diabetes Research and Training Center and CA68485 and DK20593 for the Vanderbilt Cell Imaging Resource.

REFERENCES

- Antczak, J. B., and Joklik, W. K. (1992). Reovirus genome segment assortment into progeny genomes studied by the use of monoclonal antibodies directed against reovirus proteins. *Virology* **187**, 760–776.
- Babiss, L. E., Luftig, R. B., Weatherbee, J. A., Weising, R. R., Ray, U. R., and Fields, B. N. (1979). Reovirus serotypes 1 and 3 differ in their *in vitro* association with microtubules. *J. Virol.* **30**, 863–874.
- Banerjee, A. C., Brechling, K. A., Ray, C. A., Erikson, H., Pickup, D. J., and Joklik, W. K. (1988). High-level synthesis of biologically active reovirus protein sigma 1 in a mammalian expression vector system. *Virology* **167**, 601–612.
- Belli, B. A., and Samuel, C. E. (1991). Biosynthesis of reovirus-specified polypeptides: Expression of reovirus S1-encoded sigma 1NS protein in transfected and infected cells as measured with serotype specific polyclonal antibody. *Virology* **185**, 698–709.
- Brentano, L., Noah, D. L., Brown, E. G., and Sherry, B. (1998). The

- reovirus protein $\mu 2$, encoded by the M1 gene, is an RNA-binding protein. *J. Virol.* **72**, 8354–8357.
- Brown, E. G., Nibert, M. L., and Fields, B. N. (1983). The L2 gene of reovirus serotype 3 controls the capacity to interfere, accumulate deletions and establish persistent infection. In "Double-Stranded RNA Viruses" (R. W. Compans and D. H. L. Bishop, Eds.), pp. 275–287. Elsevier, Amsterdam.
- Chelsky, D., Ralph, R., and Jonak, G. (1989). Sequence requirements for synthetic peptide-mediated translocation to the nucleus. *Mol. Cell. Biol.* **9**, 2487–2492.
- Coombs, K. M. (1996). Identification and characterization of a double-stranded RNA-reovirus temperature-sensitive mutant defective in minor core protein $\mu 2$. *J. Virol.* **70**, 4237–4245.
- Coombs, K. M. (1998a). Stoichiometry of reovirus structural proteins in virus, ISVP, and core particles. *Virology* **243**, 218–228.
- Coombs, K. M. (1998b). Temperature-sensitive mutants of reovirus. *Curr. Top. Microbiol. Immunol.* **233/1**, 69–108.
- Dales, S., Gomatos, P., and Hsu, K. C. (1965). The uptake and development of reovirus in strain L cells followed with labelled viral ribonucleic acid and ferritin-antibody conjugates. *Virology* **25**, 193–211.
- Dryden, K. A., Farsetta, D. L., Wang, G., Keegan, J. M., Fields, B. N., Baker, T. S., and Nibert, M. L. (1998). Internal structures containing transcriptase-related proteins in top component particles of mammalian orthoreovirus. *Virology* **245**, 33–46.
- Fields, B. N., Raine, C. S., and Baum, S. G. (1971). Temperature-sensitive mutants of reovirus type 3: Defects in viral maturation as studied by immunofluorescence and electron microscopy. *Virology* **43**, 569–578.
- Francki, R. I. B., and Boccardo, G. (1983). The plant *Reoviridae*. In "The *Reoviridae*" (W. K. Joklik, Ed.), pp. 505–563. Plenum, New York.
- Garcia-Bustos, J., Heitman, J., and Hall, M. N. (1991). Nuclear protein localization. *Biochim. Biophys. Acta* **1071**, 83–101.
- Gomatos, P. J., Tamm, I., Dales, S., and Franklin, R. M. (1962). Reovirus type 3: Physical characteristics and interactions with L cells. *Virology* **17**, 441–454.
- Haller, B., Barkon, M. L., Vogler, G. P., and Virgin, H. W., IV (1995). Genetic mapping of reovirus virulence and organ tropism in severe combined immunodeficient mice: Organ-specific virulence genes. *J. Virol.* **69**, 357–364.
- He, D., Nickerson, J. A., and Penman, S. (1990). Core filaments of the nuclear matrix. *J. Cell Biol.* **110**, 569–580.
- Matoba, Y., Colucci, W. S., Fields, B. N., and Smith, T. W. (1993). The reovirus M1 gene determines the relative capacity of growth of reovirus in cultured bovine aortic endothelial cells. *J. Clin. Invest.* **92**, 2883–2888.
- Matoba, Y., Sherry, B., Fields, B. N., and Smith, T. W. (1991). Identification of the viral genes responsible for growth of strains of reovirus in cultured mouse heart cells. *J. Clin. Invest.* **87**, 1628–1633.
- Mukaigawa, J., and Nayak, D. P. (1991). Two signals mediate nuclear localization of influenza virus (A/WSN/33) polymerase basic protein 2. *J. Virol.* **65**, 245–253.
- Nath, S. T., and Nayak, D. P. (1990). Function of two discrete regions is required for nuclear localization of polymerase basic protein 1 of A/WSN/33 influenza virus (H1 N1). *Mol. Cell. Biol.* **10**, 4139–4145.
- Nibert, M. L., Schiff, L. A., and Fields, B. N. (1996). Reoviruses and their replication. In "Fields Virology" (B. N. Fields, D. M. Knipe, P. M. Howley, et al., Eds.), 3rd ed., pp. 1557–1596. Raven Press, New York.
- Noble, S., and Nibert, M. L. (1997). Core protein $\mu 2$ is a second determinant of nucleoside triphosphatase activities by reovirus cores. *J. Virol.* **71**, 7728–7735.
- Payne, C. C., and Mertens, P. P. C. (1983). Cytoplasmic polyhedrosis viruses. In "The *Reoviridae*" (W. K. Joklik, Ed.), pp. 505–563. Plenum, New York.
- Rhim, J. S., Jordan, L. E., and Mayor, H. D. (1962). Cytochemical, fluorescent-antibody and electron microscopic studies on the growth of reovirus (ECHO 10) in tissue culture. *Virology* **17**, 342–355.
- Rodgers, S. E., Barton, E. S., Oberhaus, S. M., Pike, B., Gibson, C. A., Tyler, K. L., and Dermody, T. S. (1997). Reovirus-induced apoptosis of MDCK cells is not linked to viral yield and is blocked by Bcl-2. *J. Virol.* **71**, 2540–2546.
- Rodgers, S. E., Connolly, J. L., Chappell, J. D., and Dermody, T. S. (1998). Reovirus growth in cell culture does not require the full complement of viral proteins: Identification of a $\sigma 1$ s-null mutant. *J. Virol.* **72**, 8597–8604.
- Schmechel, S., Chute, M., Skinner, P., Anderson, R., and Schiff, L. (1997). Preferential translation of reovirus mRNA by a $\sigma 3$ -dependent mechanism. *Virology* **232**, 62–73.
- Sharpe, A. H., Chen, L. B., and Fields, B. N. (1982). The interaction of mammalian reoviruses with the cytoskeleton of monkey kidney CV-1 cells. *Virology* **120**, 399–411.
- Sherry, B., and Blum, M. A. (1994). Multiple viral core proteins are determinants of reovirus-induced acute myocarditis. *J. Virol.* **68**, 8461–8465.
- Sherry, B., and Fields, B. N. (1989). The reovirus M1 gene, encoding a viral core protein, is associated with the myocarditic phenotype of a reovirus variant. *J. Virol.* **63**, 4850–4856.
- Sherry, B., Torres, J., and Blum, M. A. (1998). Reovirus induction of and sensitivity to beta interferon in cardiac myocyte cultures correlate with induction of myocarditis and are determined by viral core proteins. *J. Virol.* **72**, 1314–1323.
- Spendlove, R. S., Lennette, E. H., Knight, C. O., and Chin, J. (1963). Development of viral antigen and infectious virus on HeLa cells infected with reovirus. *J. Immunol.* **90**, 548–553.
- Spendlove, R. S., Lennette, E. H., Chin, J. N., and Knight, C. O. (1964). Effect of antimetabolic agents on intracellular reovirus antigen. *Cancer Res.* **24**, 1826–1833.
- Virgin, H. W., IV, Mann, M. A., Fields, B. N., and Tyler, K. L. (1991). Monoclonal antibodies to reovirus reveal structure/function relationships between capsid proteins and genetics of susceptibility to antibody action. *J. Virol.* **65**, 6772–6781.
- Wiener, J. R., Bartlett, J. A., and Joklik, W. K. (1989). The sequences of reovirus serotype 3 genome segments M1 and M3 encoding the minor protein $\mu 2$ and the major nonstructural protein μNS , respectively. *Virology* **169**, 293–304.
- Yin, P., Cheang, M., and Coombs, K. M. (1996). The M1 gene is associated with differences in the temperature optimum of the transcriptase activity. *J. Virol.* **70**, 1223–1227.
- Yue, Z., and Shatkin, A. J. (1996). Regulated, stable expression and nuclear presence of reovirus double-stranded RNA-binding protein $\sigma 3$ in HeLa cells. *J. Virol.* **70**, 3497–3501.
- Zarbl, H., and Millward, S. (1983). The reovirus multiplication cycle. In "The *Reoviridae*" (W. K. Joklik, Ed.) pp. 107–196. Plenum, New York.
- Zou, S., and Brown, E. G. (1992). Nucleotide sequence comparison of the M1 genome segment of reovirus type 1 Lang and type 3 Dearing. *Virus Res.* **22**, 159–164.
- Zou, S., and Brown, E. G. (1996a). Stable expression of the reovirus $\mu 2$ protein in mouse L cells complements the growth of a reovirus ts mutant with a defect in its M1 gene. *Virology* **217**, 42–48.
- Zou, S., and Brown, E. G. (1996b). Translation of the reovirus M1 gene initiates from the first AUG codon in both infected and transfected cells. *Virus Res.* **40**, 75–89.
- Zweerink, H. J., Morgan, E. M., and Skyler, J. S. (1976). Reovirus morphogenesis: Characterization of subviral particles in infected cells. *Virology* **73**, 442–453.